Asia-Pac. J. Atmos. Sci., 52(3), 263-279, 2016
DOI:10.1007/s13143-015-0088-z

pISSN 1976-7633 / eISSN 1976-7951

Examination of Physical Processes of Convective Cell Evolved from a MCS - Using a Different Model Initialization

Vlado Spiridonov[1] and Mladjen Ćurić[2]

[1]*Institute of Physics, St Cyril and Methodius University, Skopje, Macedonia*
[2]*Institute of Meteorology, University of Belgrade, Belgrade, Serbia*

(Manuscript received 11 November 2015; accepted 29 January 2016)

Abstract: The present study is focused on examination of the physical processes of convective cell evolved from a MCS occurred on 4 November 2011 over Genoa, Italy. The Quantitative Precipitation Forecasts (QPF) have been performed using WRF v3.6 model under different configurations and cloud permitting simulations. The results indicate underestimation of the amount of precipitation and spatial displacement of the area with a peak 24-h accumulated rainfall in (mm). Our main objective in the research is to test the cloud model ability and performance in simulation of this particular case. For that purpose a set of sensitivity experiments under different model initializations and initial data have been conducted. The results also indicate that the merging process apparently alters the physical processes through low- and middle-level forcing, increasing cloud depth, and enhancing convection. The examination of the microphysical process simulated by the model indicates that dominant production terms are the accretion of rain by graupel and snow, probabilistic freezing of rain to form graupel and dry and wet growth of graupel. Experiment under WRF v3.6 model initialization has shown some advantage in simulation of the physical processes responsible for production and initiation of heavy rainfall compared to other model runs. Most of the precipitation came from ice-phase particles-via accretion processes and the graupel melting at temperature $T_0 \geq 0^{o}C$. The rainfall intensity and accumulated rainfall calculated by the model closely reflect the amount of rainfall recorded. Thus, the main benefit is to better resolve convective showers or storms which, in extreme cases, can give rise to major flooding events. In such a way, this model may become major contributor to improvements in weather analysis and small-scale atmospheric predictions and early warnings of such subscale processes.

Key words: Convective cell, MCS, model initialization, cloud microphysics, intense precipitation, flash flooding

1. Introduction

Convective storms are perhaps the most violent of all storm types, and are capable of producing damaging winds, large amounts of hail, heavy rainfall and weak-to-violent tornadoes. Furthermore, the fact that convective clouds often form in a line means they often group into a complex, as more of them are located close to each other. This complex is called a Mesoscale Convective System (MCS) (e.g. Ćurić, 2000; Houze, 2004). The dynamics of this system are much more complicated than those that characterise individual cumulonimbus clouds (e.g. Houze, 1993; Coniglio et al., 2007). It appears in different forms, depending on whether it occurs in the tropics or in temperate latitudes. Such areas are characterised by widespread precipitation that is partially convective and partially stratiform. Rainfall area often serves as a basic characteristic of such a complex. An important aspect in the study of convective clouds is the identification of some processes as cloud splitting or merging, which lead to intense hailfall and rainfall (e.g., Ćurić et al., 2009; Spiridonov et al., 2010; Ćurić and Janc, 2012). These processes are found to depend on the atmospheric stability, wind shear and veering, the relative stages of development of the two clouds and their initial separation. Interaction between convective cells may alter cell longevity, intensity, and propagation characteristics. Convective cloud systems are also significant from a climatological point of view (e.g., Nakazawa, 1988; Chen et al., 1996; Mathon et al., 2002). Many previous studies have focused on investigating the main characteristics of convective clouds originated from MCS's and their forecasting (e.g., Doswell et al., 1996; Nachamkin and Cotton, 1999; Fritsch and Forbes, 2001; Parker and Johnson, 2004; De Lima et al., 2005; Bresson et al., 2012; Goyens et al., 2012). In this context, a series of numerical simulations using different atmospheric models have been performed, in order to improve further understanding and knowledge concerning which processes were important in the initiation and development of the severe storms as well as which factors contributed to the associated heavy rainfall. As part of the Convective Storm Initiation Project (CSIP) Marsham and Parker (2006) studied the dynamical effects on secondary initiation of multiple bands of cumulonimbus over southern Britain. Their results imply that the thermal induced gravity waves, generated by the 'primary storm' with a three different wave modes-have been responsible for initiating the further three arcs of convective showers that were observed. They found that the fastest two modes suppressed convection and later modes increased boundary-layer depth and so initiated convection. For example, Blamey and Reason (2009) used an MM5 model to study convective system over the east coast of South Africa to examine the processes which could be contributed in

Corresponding Author: Vlado Spiridonov, Institute of Physics, St Cyril and Methodius University, Skupi 28, 1000 Skopje, Macedonia
E-mail: vspiridonov@meteo.gov.mk

initiation of intense precipitation. Their results indicate that the specific terrain structure is the main triggering factor of advection of moisture driven by low level winds as precondition of initiation of heavy persistent rainfall. In addition Clark et al. (2013a, b) studied the evolution of an MCS across southern England on 25 August 2005. Their comprehensive study focused on both observation and the modelling part with numerical simulations of MCS using 1 km resolution the Met Office Unified Model. Observation suggests presence of a weak rear-inflow jet, convergence triggered by ascent gravity waves generated by the MCS, pool merging and formation of a bow echo. A model sensitivity runs suggest that the instability is a key driving factor of the MCS promoted by an inflow jet. Both heating through glaciations and cooling through snow evaporation and the presence of ice-phase processes have a common effect on strengthening and acceleration of the system during the middle phase of the system's lifetime. The role of Planetary Boundary Layer (PBL) and microphysics (MPS) processes in reproducing the heavy rainfall event over central Korea is examined by Byun et al. (2015) using a WRF model with a set of sensitivity experiments. The main findings of this comprehensive study suggest that WRF model under specific combination of PBL and MPS schemes has shown a good skill in quantitative precipitation forecasting. Other important conclusion from their research is that the spatial resolution is dominated by PBL processes while the rainfall intensity is mainly determined by MPS.

One of the most severe a long-lasting MCS affected Genoa region on 4 November 2011 causing for about 500 mm rainfall within 6-h period and heavy flooding. Several observation and modelling studies have been focused on examination of this very specific atmospheric case. For example Pulvirenti et al. (2011) applied an automatic method using data provided by the Earth Observation Satellite System-Cosmo-Sky Med in order to detect flooding. Parodi et al. (2012) presented an overview of the meteorological conditions responsible for initiation of flash flooding. For example Silvestro et al. (2012) analysed the same severe case by applying hydro-meteorological probabilistic modelling to a small affected catchments area, while Mrowiec et al. (2012) used different dynamical and microphysical cores to analyse three cloud-resolving model simulations of a strong convective event observed during the TWP-ICE campaign. Their comparative analysis of the radar reflectivity shown a relatively good agreement between modelled and observation of convective and stratiform precipitation areas. They also found that convective updrafts are fairly consistent across simulations with exception to hydrometeor loading which differs significantly. It is also found that convective downdrafts mass fluxes vary substantially below a melting layer and all convective and stratiform downdrafts contain precipitation below 10 km and nearly all updrafts are cloudy above the melting level. Their conclusions give a good basis for further examination of the microphysical parameterizations.

In addition, Schenkman et al. (2012) ran the ARPS prediction system to simulate a tornados' mesovortex that developed within an MCS. Based on their findings the main triggering factor of initiation of mesovortex is a strong low-level updraft that is critical of convergence and acceleration of the vertical vorticity. Results obtained by the vertical cross sections also reveal that updraft represents a strong rotor where the horizontal vorticity evolves in the near surface inflow caused by surface friction.

van Weverberg et al. (2013) examined the role of microphysical parameterisation in the simulation of MCSs in the tropical western Pacific. Results in general indicate that microphysics parameterization plays a crucial role in simulation of the convective system. While there is no obvious improvement of using a double moment microphysics scheme-since explicit prediction of number concentration does not necessarily improve some microphysical processes e.g. ice nucleation, accretion and sedimentation. In addition they found an overestimation of the precipitation at the surface-which is not to much sensitive to the microphysics scheme used in the present study. Rebora et al. (2013) analysed the role of certain factors (e.g. synoptic situation, unstable air mass, moist low-level jet and topography) for developing of severe rainfall processes. For their analysis authors used remote sensing technique (the Italian Radar Network mosaic, Meteosat Second Generation, Moderate Resolution Imaging Spectroradiometer and the Italian rain gauge network observations). Their work also addressed the possible role of sea-atmosphere interactions and proposes a characterization of these events in terms of predictability of heavy rainfall in MCS. Both analysis events associate with heavy flooding have some consistency e.g. the creation of positive vertical vorticity, strong south-western flow which triggers the precipitation, heavy rainfall amount and small affected area. Their results also re-affirmate the role of the synoptic scale system on development of specific mesoscale atmospheric pattern associate with landward advection of warm and moist air which rotates clock-wise and intensifies with height, low level convergence, specific orographic lifting, blocking by stationary high pressure over central Europe. These ingredients were mainly responsible for initialization and initiation of strong persistent autogenerating V-shape heavy rainfall structure causing flooding over small area over Genoa. The modelling study for this specific case is carried out by Fiori et al. (2014) using a non-hydrostatic ARW-WRF model with different microphysics schemes to study the physical processes responsible for such heavy rainfall resulting from the finger-like convective system, as well as to compare their results with observations. Their results suggest that this particular atmospheric phenomenon strongly depends on both the mesoscale initialization and the microphysical parameterization, which has impact on initiation of heavy rainfall. Recently, Buzzi et al. (2013) analyzed the main dynamical processes responsible for initiation, evolution and lifecycle of convective systems responsible for intensive precipitation over Liguria Sea, using non-hydrostatic MOLOCH model. In addition the ability of this model for QPF has been tested using different model resolutions.

The objective of this study is to examine the ability of cloud model to simulate the main physical processes during the most intense phase of convective cell originated (evolved) from MCS that occurred over Genoa on 4 November 2011. Our main focus is to test the model capability and performance in examination of the physical processes of this particular convective cell to various initializations. More specifically the objective is to analyse the certain microphysical processes responsible for initiation of heavy convective rainfall and flooding using a high resolution three-dimensional model runs. First, an overview on the synoptic situation surrounding the 4 November 2011 MCS is given. The experimental setup including model initialization and initial conditions are explained in the next section. The results of the model simulation, presented in Section 4 are discussed in light of the microphysical sensitivity and in respect to the comparison with observation.

2. Model formulation and description

a. Cloud model

The convective cloud model is a three-dimensional, non-hydrostatic, time-dependant, compressible system that uses the dynamic scheme from Klemp and Wilhelmson (1978). The thermodynamic energy equation is based on Orville and Kopp (1977), with the effects of the snowfield added. The bulk microphysical parameterisation follows Lin et al. (1983).

The present version of the model contains ten prognostic equations: three momentum equations, the pressure and thermodynamic equations, four continuity equations for the water substances, and a subgrid-scale kinetic energy equation. All equations are specified in the Cartesian co-ordinate system. More information regarding the model can be found (e.g. Telenta and Aleksic, 1988; Spiridonov and Ćurić, 2003, 2006).

b. Dynamics and thermodynamics

The dynamical part of the model is based on the pressure equation and the compressible equations of motions. These equations are derived from the Navier-Stokes equations, using Boussinesq approximation for the homogeneous and rotating fluid, taking into account advection, turbulent transport, buoyancy and pressure gradient force. Boundary-layer (or vertical mixing) is covered by the use of Turbulent Kinetic Energy (TKE) scheme. The pressure equation is derived by combining the compressible continuity and thermodynamic equations. Initial and boundary conditions and numerical technique are based on Durran (1981) and Klemp and Durran (1983). Model uses homogeneous meteorological fields with artificial initiation of convection, using a thermal bubble and temperature perturbation. Thus radiation scheme and topography are not included into the current version of the model.

c. Cloud microphysics

Bulk water parameterisation based on Lin et al. (1983) is used to simulate microphysical processes. It uses a single-moment scheme for the six water categories: water vapour, cloud water, cloud ice, rain, snow and graupel or hail. Cloud water and cloud ice are assumed to be monodisperse, with zero terminal velocities. Rain, hail and snow have the Marshal-Palmer type size distributions with fixed intercept parameters. The source references for the scheme to allow for the co-existence of cloud water and cloud ice in the temperature region of -40^{o}C to 0^{o}C (e.g. Hsie et al., 1980). Rather than using the hail spectrum from zero to infinity (idealised spectrum), (e.g., Ćurić and Janc, 1995; 1997) proposed considering the hail size spectrum, which only includes hail-sized particles (larger than 0.5 cm in diameter; hereafter called the realistic hail spectrum). Four prognostic conservation equations for the exchange of water substances are considered in the model. One of the prognostic variables is the sum of the mixing ratios for water vapour, cloud water and cloud ice. Other prognostic variables are the mixing ratios of rain, graupel or hail and snow. The equivalent radar reflectivity factors for hail and rain are computed by the equations given by Smith et al. (1975) and empirical equation for snow by Sekhon and Srivastava (1970).

d. General observational analysis

The heavy rainfall event was observed over Genoa-in Liguria region on the northwest coastline on the Mediterranean sea-Italy on 4 November 2011. The main target area affected by this flash flooding event is the Fereggiano sub-basin located in the centre of Liguria region passing through Genoa city. A set of data provided by the Italian official observation network (ICPD) with semi-professional network (LIMET) and the meteorological radar (see Figs. 1a-c) allowed to well document of heavy rainfall from 0900 to 1500 UTC influenced by a persistent-finger-like isolated and auto-regenerating convective structure. A daily local maximum evidenced by LIMET PWS "Quezzi", located in the Fereggiano area was about 556 mm. The maximum rainfall depth registered in 1 h at the same station from 1100 to 1200 UTC was 166 mm. Figure 1a shows the observed features of rainfall depth registered by the official Italian rainguage network (ICPD). According to the rainfall measurements at Gavette and Campo Liguria stations (see Silvestro et al., 2012), an hourly maximum rainfall intensity of 120 and 165 mm h^{-1} was registered between 1100 to 1200 UTC (Fig. 2b). The lifecycle of this particular case was continuously monitored by the Italian radar network Silvestro et al. (2012), showing the persistence of the intense convective cell moving along the Liguria coastline where reflectivity was continuously above 40 dBZ. At 1200 UTC on 4 November 2011, reflectivity at $z = 2.0$ km m.s.l. indicates a finger-like isolated and regenerative convective cell oriented along a southwest-northeast line, with an anvil spreading to the east-

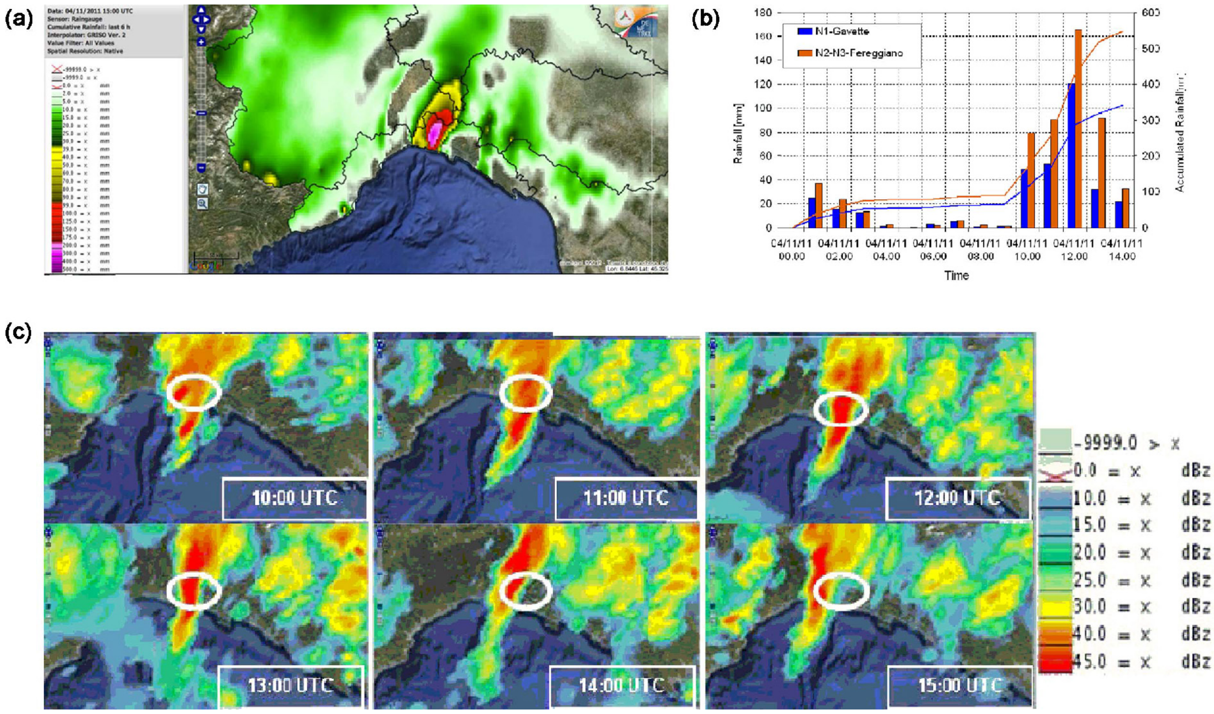

Fig. 1. (a) Total rainfall depth between 0900 and 1500 UTC, as provided by the ICPD raingauge network. (b) Hourly rainfall intensity and total accumulated rainfall for three rain gauges stations observed in the Gavete and Fereggiano sub-basin located close to the Liguira-Genoa. (c) a) Reflectivity in (dBZ) at 2.0 km height from 1000 to 1500 UTC 4 November 2011 as provided by the Italian radar network composite.

northeast (Fig. 1c). The convective structure started wandering along the eastern coast of Liguria and finally became stuck over the western hills of Genoa, producing torrential rainfall. A well organised and regenerating finger shape MCS remained stationary for a signicant number of hours over the Liguria coastline, causing very high rainfall and flooding over Genoa. This MCS produced an embedded convection with high precipitation convective structure that evolved into a rotating comma head pattern.

As it is displayed in Fig. 2a the model configurations consists of an outer domain with 20 km grid (domain 1) and four nested domains with 10 km, 5 km, 2.5 km and 1 km grid resolution, respectively. The inner shaded box is domain 5 (1 km) covering the central part of Liguria-Fereggiano sub-basin, where heavy rainfall occurred. Figures 2b-e depict the basic weather charts obtained from WRF v3.6 model using the initial and 6 hourly lateral boundary conditions forced by the NCEP FNL data on $1^{o} \times 1^{o}$ degree grid resolution without specific data assimilation. The synoptic scale system located over Western Europe, characterized by a deep low-pressure structure and atmospheric baroclinity, generating a jet stream with positive vorticity advection with a south-westerly flow over the Liguria Apennines ridge at 500 hPa (Fig. 2b), an intense moist SW-NW streamflow towards Liguria Apennines (Fig. 2c) and low level convergence of the two air masses (Fig. 2d), strong pressure ridge centred on Eastern Europe that acted as a block to the motion of this system, which also encountered an anomalously warm western Mediterranean Sea (Fig. 2c), thus increasing the potential severity of the cyclone by strongly moistening the low-level troposphere. The particular synoptic pattern identifies several important features that were responsible for development of MCS and initiation of heavy rainfall and flooding. The addition thermodynamic and instability factors include: a moist layer of sufficient depth in the lower-to-mid troposphere, instability and source of lift, wind veering at the near-surface layer, and wind shear with a relatively large values of CAPE and LI (Fig. 2e). The observed event appears to be a Mesoscale Convective System (MCS) formed at a quasi-stationary low-level convergence line, with steady low-level moisture supply off the coast feeding into the front, causing flash flooding (Silvestro et al., 2012).

e. WRF v3.6 model setup and experimental design

The first set of experiments has been performed using 3.6 version of the WRF model. Table 1 illustrates the model configurations adopted over five model domains displayed on Fig. 2a. The entire grid system has been discretized in 28 levels specified on the standard pressure coordinates. The rainfall forecast was very sensitive to the model initialization, treatment of convection, horizontal resolution and the microphysics parameterization scheme (MPS). The initial fields and boundary conditions with 6 hourly updates taken from the National Centers for Environmental Prediction (NCEP) Final

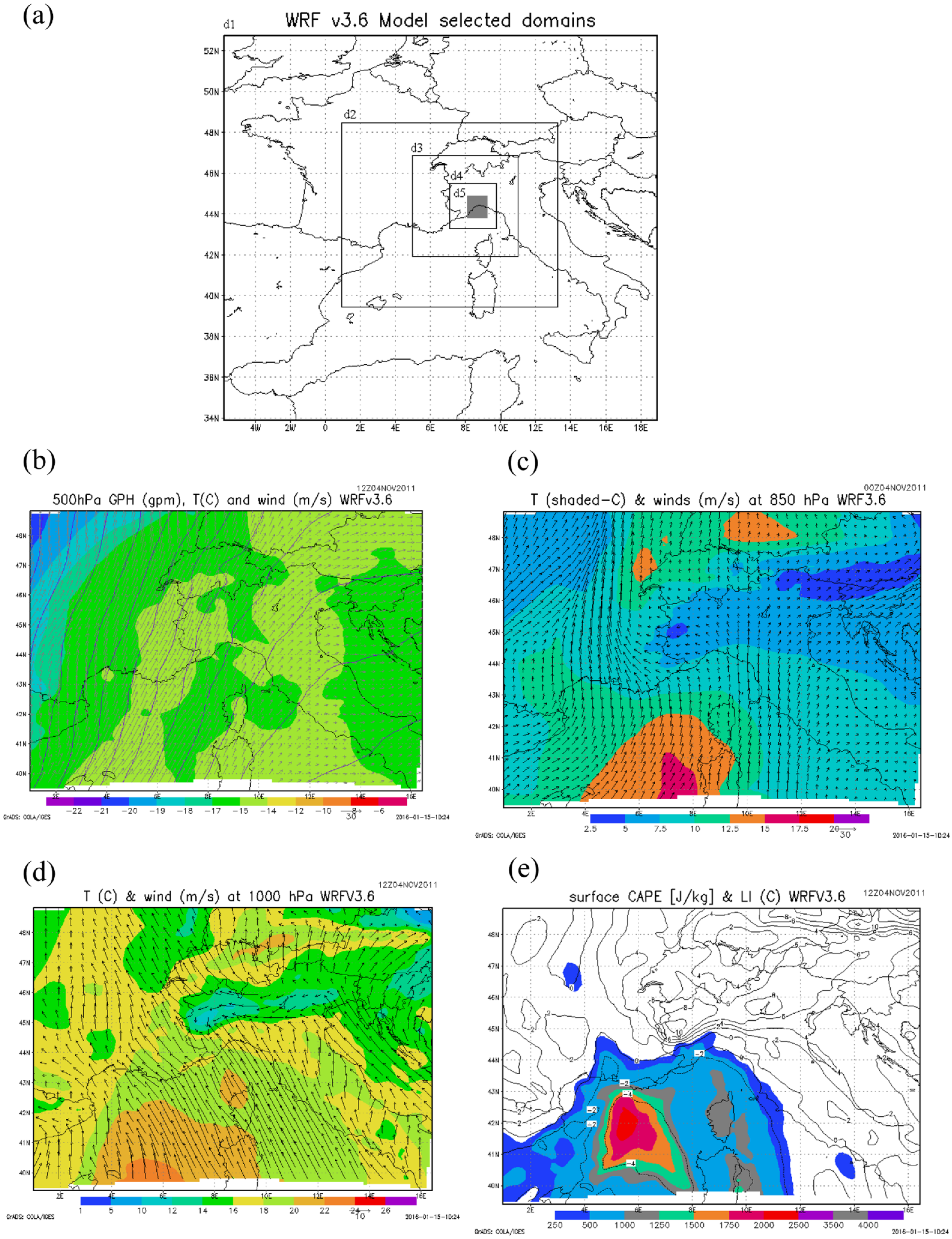

Fig. 2. (a) The model selected domains. The outer box is domain 1 (20 km). The inner boxes denote the domain 2 (10 km), domain 3 (5 km) domain 4 (2.5 km) and domain 5 (1 km), respectively, (b) 500-hPa geop.height in (gpm) map at 1200 UTC 4 November 2011. WRF-v3.6 forecast with 10 km grid resolution (domain 2), (c) Same as Fig. 1b but for 850 hPa, (d) Convergence line. 2-m temperature (°C), 10-m wind vectors (full barb denotes 20 m s^{-1}) at 1200 UTC 4 November 2011, and (e) Convective Available Potential Energy-CAPE (J kg^{-1}) and lifted index (°C) valid at 1200 UTC 4 November 2011.

Table 1. WRF v3.6 model setup and 24-h accumulated precipitation (mm) for all sensitivity experiments.

Model setup/Run	Model initialization and forecast duration	Horizontal resolution (km)	Time step (s)	Domain Grid points	Microphysics	Cumulus scheme convection	Total accumulated rainfall (mm)
(a) Experiment 1	0000 UTC 4 Nov. 2011 24-h	20	36	d1 66 × 100	WSM6	Betts-Miler-Janjic	121
(b) Experiment 2	0000 UTC 4 Nov. 2011 24-h	10	18	d2 66 × 100	WSM6	Betts-Miler-Janjic	119
(c) Experiment 3	0000 UTC 4 Nov. 2011 24-h	5	10	d3 66 × 100	WSM6	Betts-Miler-Janjic	125
(d) Experiment 4	0000 UTC 4 Nov 2011 24-h	2.5	4	d4 66 × 100	WSM6	Explicit	177
(e) Experiment 5	0000 UTC 4 Nov. 2011 24-h	1	2	d5 50/70	WSM6	Explicit	377
(f) Experiment 5	0000 UTC 4 Nov. 2011 24-h	1	2	d5 50/70	Ferrier	Explicit	380

Analysis (FNL) with a resolution of $1^o \times 1^o$. The experiments were performed for 24-h starting at 0000 UTC 4 November 2011. Figures 3a-f show 24-h accumulated rainfall (mm) for each sensitivity experiments valid at 0000 UTC 5 November 2011. Some tests were also performed with NCEP FNL data but with initialization on 3 November 2011 at 1200 UTC (not shown), but the results were not satisfactory. Almost all model runs with except to experiments 5 and 6 underpredict the 24-h accumulated rainfall (see last columnin Tab, 1). The model runs obtained with 1 km grid resolution and explicit calculation of convection by use of WSM6 and Ferrier microphysics, predicted about 377 and 380 mm 24 h accumulated rainfall, respectively. Figures 3e, f also indicate that the WRF model with this configuration is capable of reproducing the structure of convective system associate with heavy rainfall. However both experiments show a spatial displacement of heavy rainfall area for about 15-20 km to the west, which is similar result found in Fiori et al. (2014). It is also interesting to mention that the quantitative result coincides well with the total rainfall depth of 362 mm registered at ICPD “Gavette” station, while the same model predictions tend to underestimate the total maximum accumulated rainfall (556 mm) observed at LIMET-PWS “Quezzi” station as indicated in Bedrina et al. (2012). The time evolution of hourly rainfall for the Fereggiano sub-basin (domain 5) obtained from ICPD “Vicomorasso” (dash blue), ICPD “Gavette” (dash red) and LIMET PWS “Quezzi” (dash pink) and model with WSM6 (solid orange) and Ferrier (solid yellow) are depicted in Fig. 4. While the 1 km grid experiments quite reasonable capture the 24-h accumulated rainfall amount, the temporal evolution of hourly rainfall shows a large differences between modelled and observed distributions. It is evidenced that observed precipitation peaks at three stations registered from 1100 to 1300 UTC at most intense phase of evolution is missing in the model results, i.e. three peaks are not reproduced and the rain intensity is highly underestimated by the model. Table 2 gives the quantitative validation of hourly precipitation forecast using BIAS and RMSE obtained for domain 5 with WRF v3.6 forecasts with 1 km grid and explicit calculation of convection using Ferrier and WSM6 microphysics valid at 0000 UTC 4 November 2011. The values in Table 2 suggest that both prescribed microphysics, indicate a high negative Mean Algebraic Errors (BIAS’s) as measure of overall reliability, with exception to ICPD “Gavette” case where hourly forecasts of precipitation in WSM6 and Ferrier runs are biased about 0.6 and 0.8, respectively. There are large errors in hourly forecasts of precipitation in both runs, the highest being in heavy rainfall period from 1100 to 1400 UTC. Consequently, the square errors are high the measures of overall accuracy of root mean square error (RMSE) from 30-50 is much higher than the biases. This implies that some localized environmental forcing is responsible for initiation of heavy rainfall episodes-which are not correctly captured by synoptic scale processes. Another possible explanation of this underestimation is probably due to the spatial-temporal scales of the convective processes and the observed convective cell with a heavy rainfall amount that is confined in a very small area of 93 km^2, a length of 25 km and duration time of 2 h (e.g. Bedrina et al., 2012; Fiori et al., 2014). Sensitivity (e.g., Giorgi, 1990; Christenses, 2007) experiments with a finer horizontal resolution showed a relatively improved forecast skill, compared to the runs with coarser resolution. One of the possible improvements of the proper representation of heavy rainfall event could be achieved by particular combination of PBL and MPS schemes as it is suggested by Byun et al. (2015). However, some severe convective scale episodes associate with heavy precipitation could

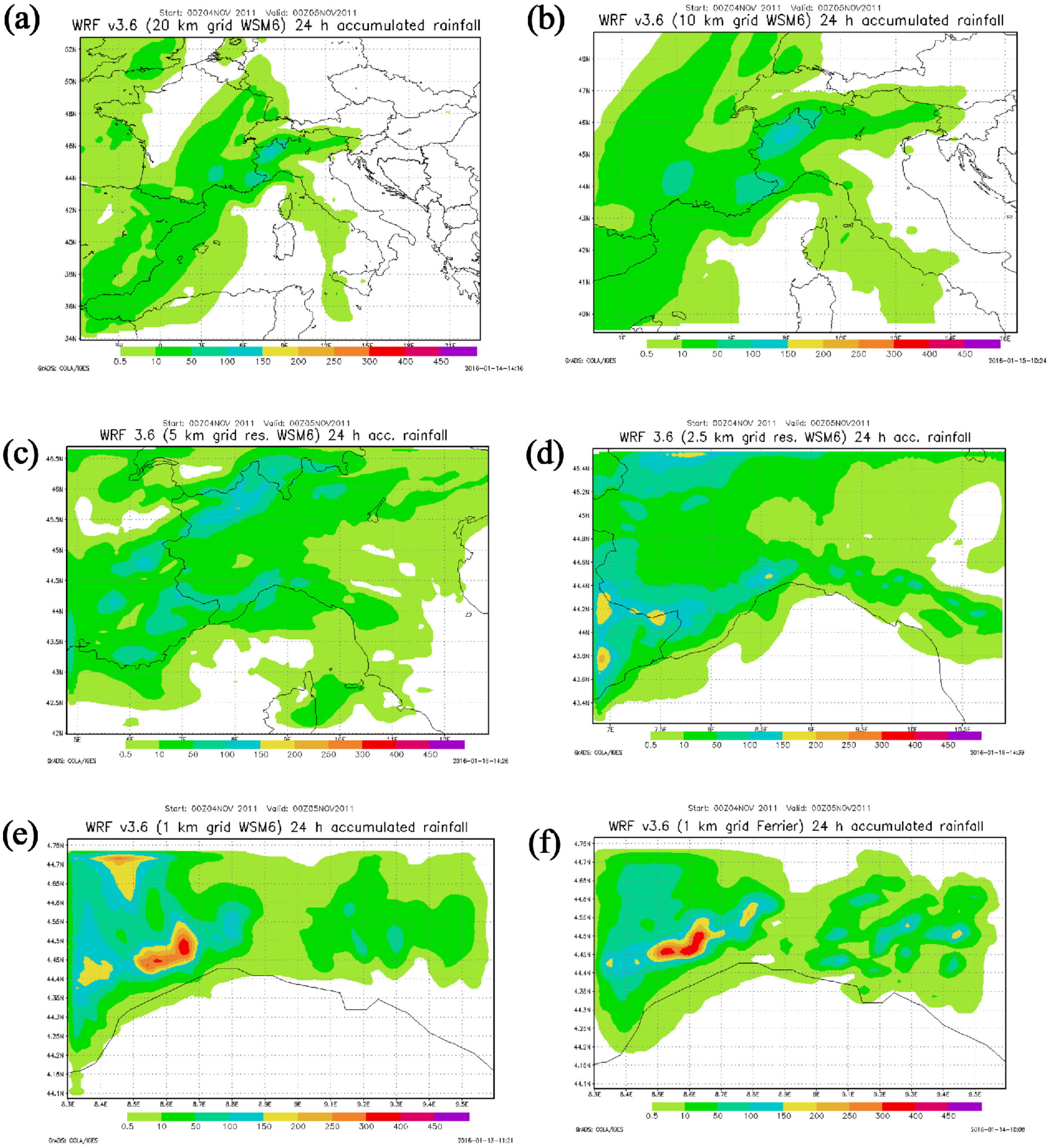

Fig. 3. WRF v3.6 24-h accumulated rainfall (mm) valid at 0000 UTC 5 November 2011. (a) 20 km grid resolution and WSM6 microphysics scheme, (b) Same as Fig. 3a but with 10 km grid, (c) Same as Fig. 3a but with 5 km grid resolution, (d) Same as Fig. 3a but with 2.5 km grid and explicit treatment of convection, (e) Same as Fig. 3d but with 1 km grid resolution, and (f) Same as Fig. 3e but using Ferrier microphysics parameterization.

not be completely resolved. Accurate forecast of such small-scale atmospheric processes which are on sub-scale model domain is still a big challenge for NWP models. It requires availability of high computer performances, a proper model configuration and setup, quality of initial data and boundary conditions and data assimilation. Some thoughts go towards identifying a key algorithm or developing some coupling method capable of producing significantly more realistic and spatially accurate forecasts of convective rainfall events, that is limited with current operational systems.

f. Cloud model initialization and initial meteorological input

An attempt has been made in this study to investigate the ability and performance of a convective cloud model to predict the Genoa heavy rainfall event. The analysis refers to the

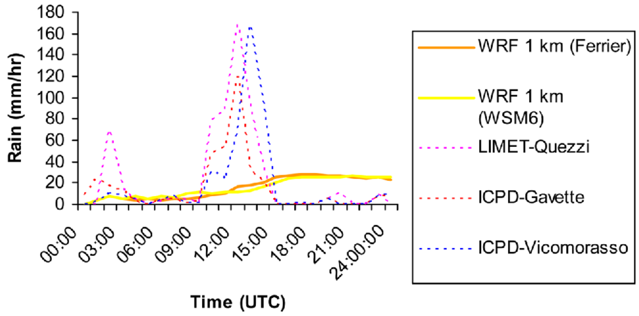

Fig. 4. The time evolution of hourly rainfall for Ferggano sub-basin (marked as a shadow box in Fig. 2a, obtained from observation at three rainguage stations (dash) and model domain 5 (dotted) box.

Table 2. Quantitative validation of hourly precipitation forecast by calculation of BIAS and RMSE for cloud permitted WRF v3.6 forecasts valid at 0000 UTC 4 November 2011, with 1 km grid and explicit calculation of convection using Ferrier and WSM6 microphysics.

Model/AWS	ICPD "Vicomorasso"		ICPD "Gavette"		LIMET PWS "Quezzi"	
WRF v3.6 1 km grid	Ferrier	WSM6	Ferrier	WSM6	Ferrier	WSM6
BIAS	−2.8	−2.8	0.8	0.6	−7.3	−7.5
RMSE	39.4	37.2	30.0	30.0	45.0	49.0

period from 1100 to 1400 UTC, during most intense phase of evolution of convective cell. As this particular event is strongly sensitive to the detail mesoscale initialization, our approach is to employ a four different initialization approaches for this experimental setup. The first and second model runs are initialized on upper air soundings for Cuneo and Milano, third model run with upgrade algorithm utilizes two upper air soundings as initialization taken from University of Wyoming (Fig. 5) and the last sensitivity experiment is initialized on WRF model output data (Fig. 6). All sensitivity runs have the consistent initialization time at 1200 UTC on 4 November 2011. The Cuneo sounding is located SW of providing meteorological input in the inflow region of the MCS with more maritime environmental characteristics. Milano sounding describes the atmospheric conditions north-westerly of the mesoscale system representing more continental features. In third model setup-instead of using initial conditions-there is an evolution of the model from the state described by one sounding and then evolving towards the other sounding. Since the storm movement is slightly shifted towards right from the main troposphere wind blowing from SW to NE, the location of the first sounding is found in the left corner of the model integration domain. The first sounding profile is taken at the time before initiation of severe convective storm evolved from MCS (Fig. 5a). The second data set is positioned upstream the heavy rainfall location at a diagonal distance of about 50 km from the first (Fig. 5b). The two soundings are starting from the same height of 250 m which is the first vertical grid point

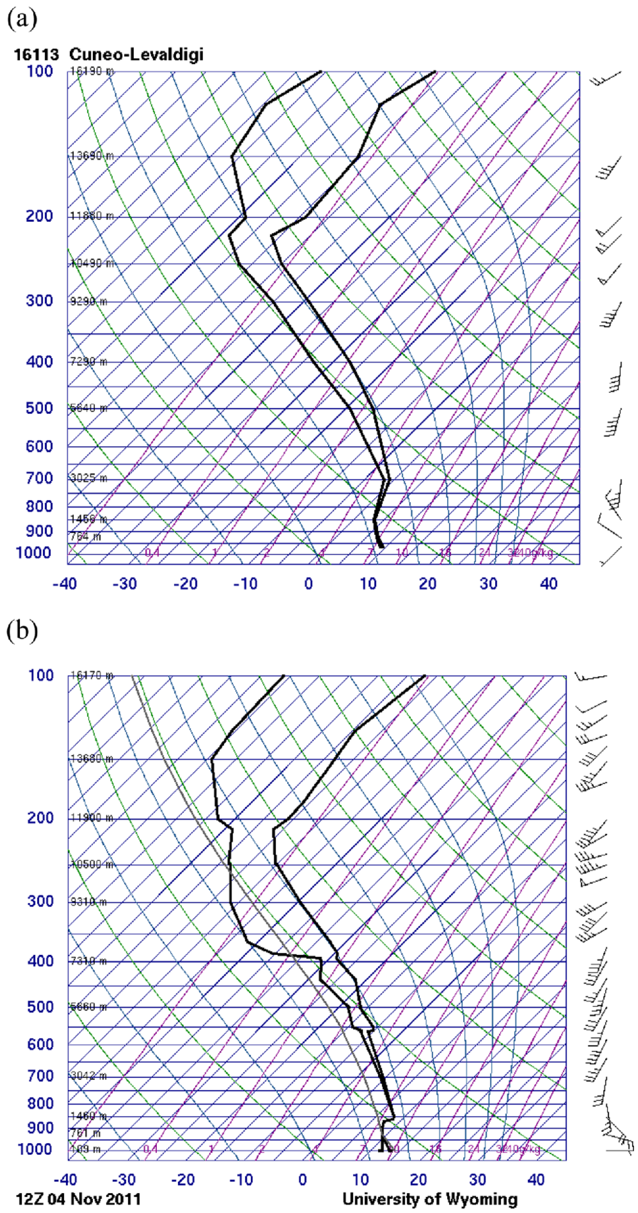

Fig. 5. (a) Upper air sounding for Cuneo-Levaldigi at 1200 UTC 4 November 2011 taken from University of Wyoming, (b) Same as for Fig. 2a but for Milano at 1200 UTC 4 November 2011.

in the model. The vertical stratification of the atmosphere (potential temperature, specific moisture and the horizontal velocity components) creates the initial input for running the model. Both soundings identify several important instability features that might be responsible for the initiation and evolution of this severe weather event. The main characteristic of upper-air soundings is increase moisture content of sufficient depth in the lower-to-mid troposphere, slight moisture deficit at upper levels. The wind profiler shows instability and source of lift, wind veering at the near-surface layer, and strong directional wind shear in a deep layer. The last initialization method utilizes the WRF forecast of upper air sounding located in the central portion of the cloud model domain. The

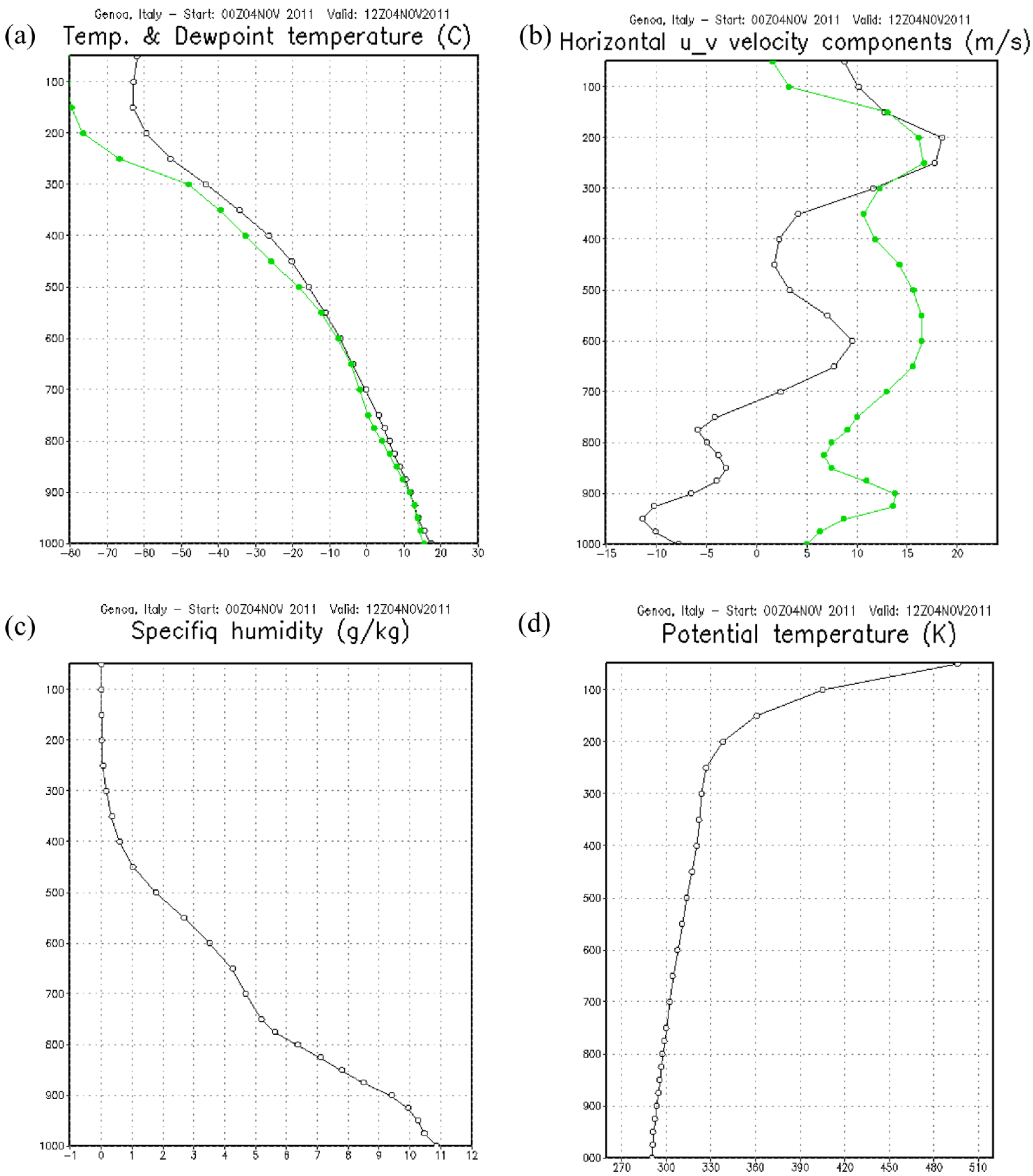

Fig. 6. Initial vertical profiles of (a) temperature and dew point temperature (°C), (b) horizontal-velocity components (m s^{-1}), (c) specific humidity (g kg^{-1}) and (d) potential temperature (K), for Genoa (lat/lon = 44.41/8.93 valid at 1200 UTC 04 November 2011 obtained with WRF v3.6 model.

initial vertical profiles of horizontal **u** and **v** velocity components in (m s^{-1}), specific humidity (g kg^{-1}) and the potential temperature (K) as meteorological input of Genoa case are depicted in Figs. 6a-d.

The initial impulse for convection is the ellipsoidal thermal bubble positioned 15 km to the left in the central portion of the cloud model domain, at a height of 2.0 km. The radial dimensions of the bubble are $x^* = 15$ km, $y^* = 15$ km and $z^* = 3.5$ km, respectively. The temperature and velocity perturbations respectively have maximum values in the bubble's centre and exponentially decrease towards zero at the bubble's boundaries. The advantage in cloud model initialization with WRF output data is that that there is no need of temperature perturbation-thus the initiation of convection is not more influenced by the modeller. Since the heavy rainfall occurs over small area less than 50×50 km^2, we choose a quite similar domain for running the model which covers $81 \times 81 \times 20$ km^3 with grid resolution of $0.5 \times 0.5 \times 0.25$ km^3. The temporal resolution of the model for integration of the model is 5 s, and a smaller one is 1 s, for solving the sound waves. The

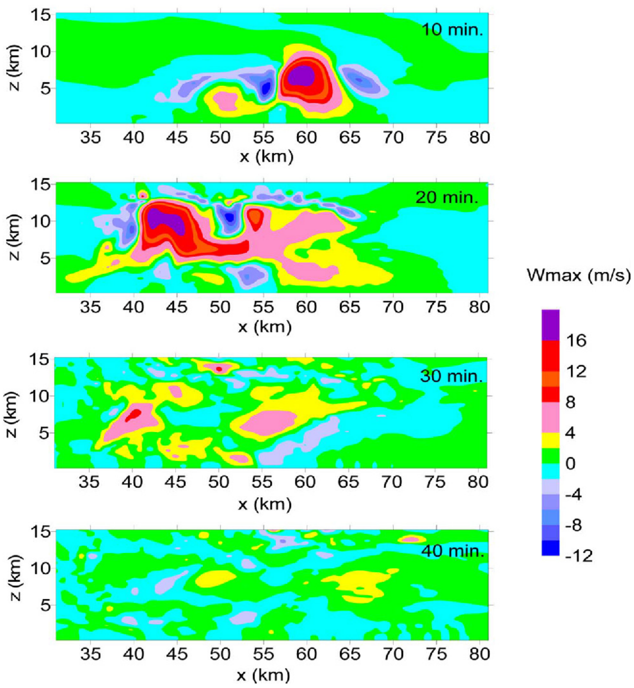

Fig. 7. The vertical distribution of updrafts and downdrafts (m s^{-1}) at cloud developing phase, from 10-40 min of the simulation time.

time duration of the numerical simulation is extended to 3 hours.

3. Model results

a. Some dynamical characteristics of the convective cell

The first part of this section starts with evaluation of some dynamical features of the simulated convective storm using WRF initialization for initiation of convection. As can be seen from Fig. 7, the simulated severe storm is characterised by the formation of a continuous pair of updrafts and downdrafts over a period longer than 30 min. One can see that the strong updraft region is initially found on the forward flank (front) of the storm. The updraft speed increases from the cloud base to the level that spreads to the middle portion of the cloud and its upper boundary. The maximum vertical velocity in the front updraft region is found to be 19.7 m s^{-1} at 6.25 km height. At 20 min the forward updraft core weakens, while a strong updraft core occurs at the back of the storm. The forward-flank downdraft with cold, dense air descends through the front of the storm in the rainfall zone, with a maximum velocity of 12 m s^{-1}. The rear-flank downdraft of cold, dense air descends through the back of the storm.

Figure 8 shows the vertical cross-sections of the cloud evolution together with a wind field from 10 to 40 min of the simulation. The main characteristic of the wind profile is that it veers or turns clockwise with altitude and wind shear at the upper levels, which are the most ideal conditions for severe convection to form. This change in wind speed and direction

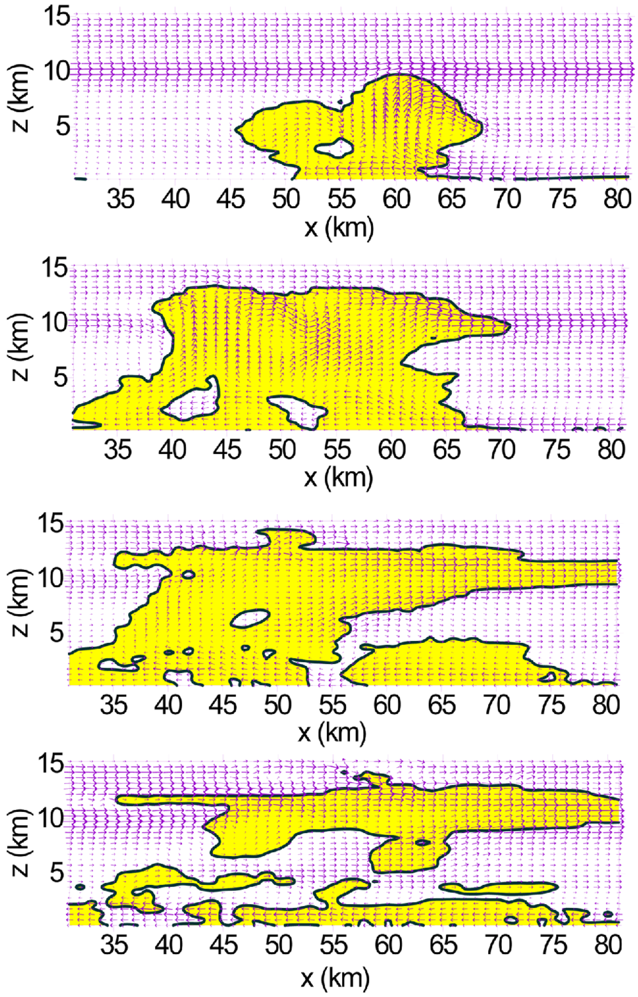

Fig. 8. The vertical cross sections of cloud the wind field during the most intensive life cycle of storm from 10 to 40 min of the simulation time with 10 min time intervals. The cloud outlines (bold lines) represent the cloud water +cloud ice mixing ratio 0.1 (g kg^{-1}).

produces storm-scale rotation, meaning the entire cloud rotates and the turning of the winds at high altitudes helps the convective system to develop its most essential component: the mesocyclone. As can be seen at the initial stage, a wide stream enters from the right front side (as viewed in the direction of movement). The moist air is rising upwards to the level of convection, before turning in an anticyclone direction in the anvil area. Air from the strong updrafts diverges at altitude in all directions. However, most of the air flows into the downstream anvil. In strong wind shear, air that flows with the wind soon adjusts to the surrounding flow and continues to move along the edge of the anvil downstream. Strong winds in the upper troposphere, which are typical of intense supercell storms, generate a long anvil with wide bands of cirrus clouds. Downdraft currents start from the middle portion of the cloud and descend in the backward flank. One of the most interesting features of the simulated storm as part of the MCS is the double vortex circulation that appears at 10 min of the

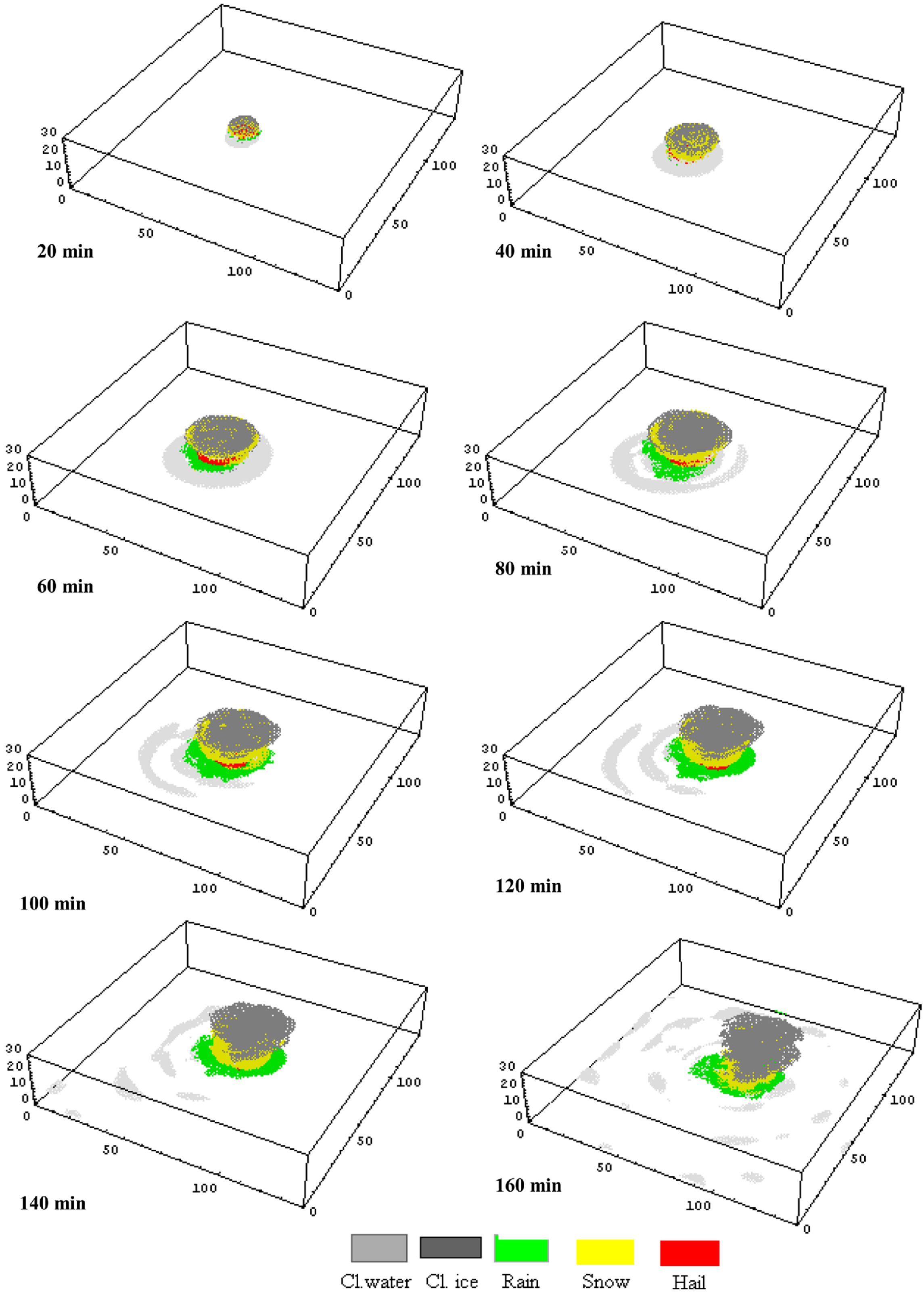

Fig. 9. A 3-d depictions of the cloud life cycle-viewed from SW to NE at 20 min intervals starting at 20 min simulation time.

simulation. The cloud model captures some dynamical features responsible for development and initiation of heavy precipitation event in the span of around 2-3 hours, during the most intensive stage of the long-lived of MCS. At 1200 UTC, a SW-

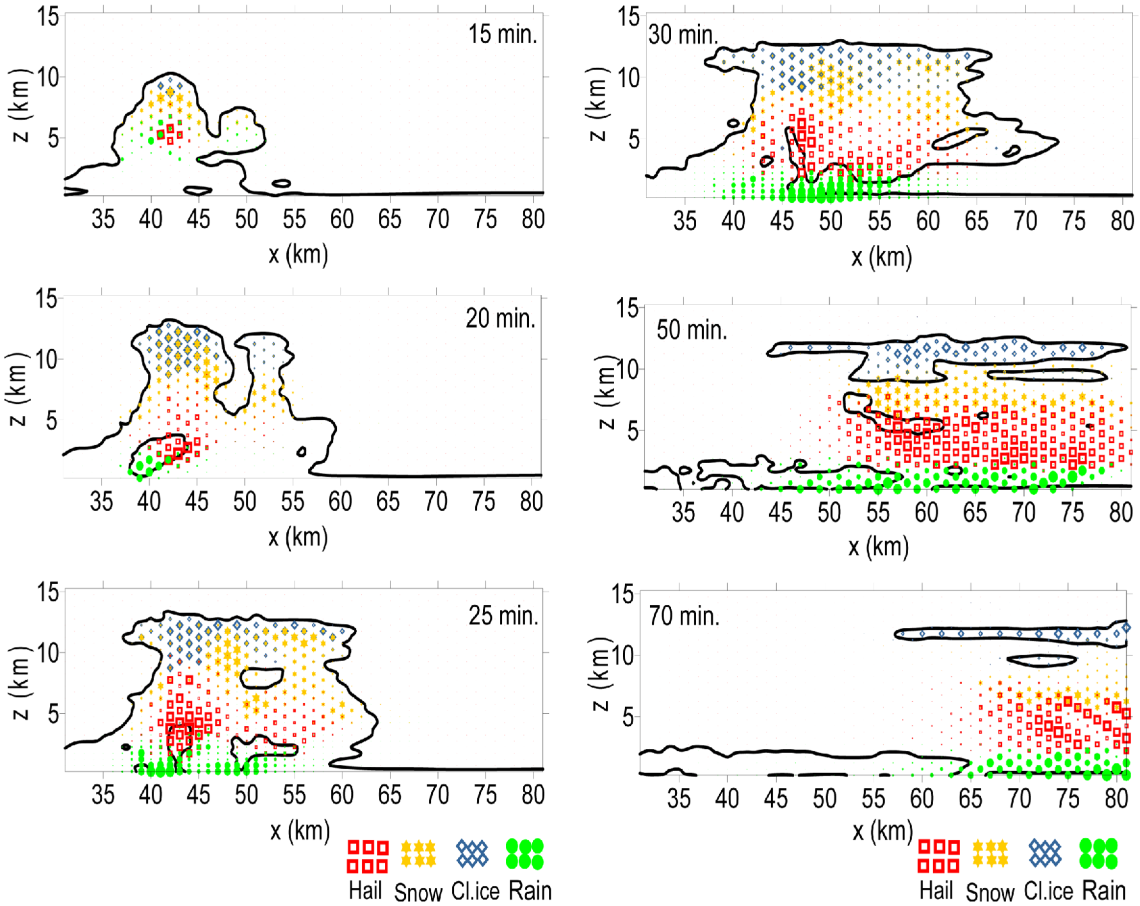

Fig. 10. (a) Vertical cross section of the microphysical structure of storm in 15, 20, 25, 30, 50 and 70 min of the simulation time. Black contours denote the cloud outline with mixing ratio greater than 0.1 g kg^{-1}.

NE oriented line of convection had developed in Genoa along the simulated frontal boundary. The cloud model was also capable of simulating the vortex circulation around the cloud and the thermally induced gravity waves by the latent heat released during the storm developing stage (see also Marsham and Parker (2006)). The vortex rings with horizontal vorticity components result from the symmetric horizontal pressure gradient in the thermal bubble. This vortex current also appears in the downdraft region, when descending air from the back of the storm spills onto the ground, causing an eddy motion. Horizontal eddy currents generated by wind shear in the near-surface layer lift up in the area of strongest convection. This initiates the transformation of the horizontal component of vorticity into a vertical, positive and negative vorticity. The maximum vorticity perturbation occurs in the region with maximum vertical velocity. A three-dimensional view of the simulated case occurred over Genoa provides a more realistic information about the storm structure and evolution. Figure 9 gives a three-dimensional depiction of the storm life cycle viewed form SW to NE at 20 min intervals starting at 20 min of the simulation. The convective cloud starts its development with the appearance of three individual cells. In this developing stage the convective cells interact and gradually enter the merging phase. After the cells merge, the cloud exhibits more intense growth and changes in its internal dynamical and microphysical structure. This merging process intensifies the cloud growth and increases the rainfall at ground level. In the most intense phase, individual cells are splitting and merging. These processes enhance the convection and alter the dynamical and microphysical structure. This storm has a typical supercell form, with wider horizontal spreading and the formation of an anvil shape, complex dynamic vortex circulation, and appearance of the gravity waves induced by latent heat release in the storm developing stage from 40 to 60 min of the simulation time. In the storm's mature stage, mesoscale stratiform precipitation forms, this consists of weakening active cloud cells, stratiform clouds and precipitation.

b. The examination of the microphysical processes

The present research continues with detailed analysis of the storm's microphysical structure and the processes which contribute to formation and initiation of intense precipitation. The vertical distribution of different hydrometeor fields during

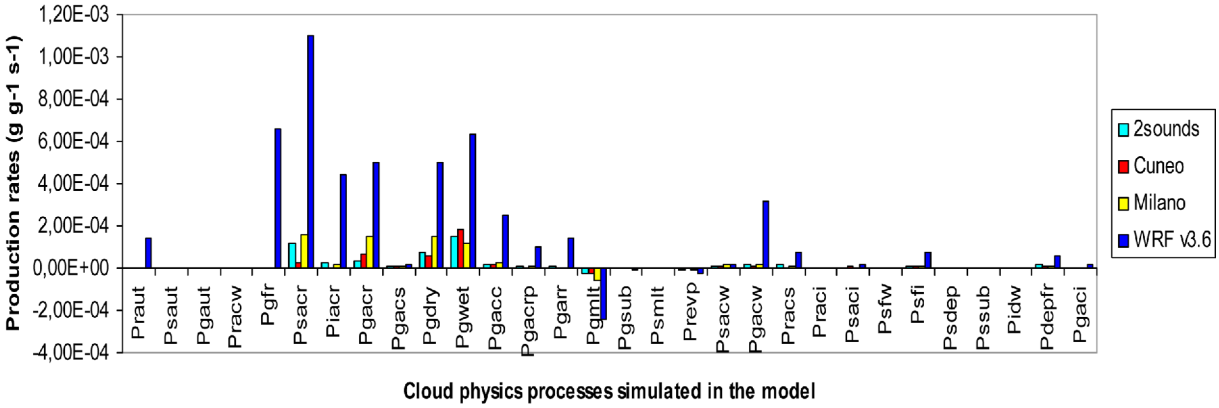

Fig. 11. Colum distribution of the mean transfer production rates of the microphysical processes-expressed through the mixing ratio of water vapor, cloud water, cloud ice, rainwater, snow and hail (g kg^{-1}), averaged over 3 h simulation period starting at 1200 UTC 4 November 2011 using a different cloud model initialization (a) A two soundings-(green bar), (b) Cuneo sounding (red), (c) Milano sounding (yellow), and (d) WRF v3.6 (blue).

simulation time is illustrated on Fig. 10. Cloud outline depicts cloud water mixing ratio greater than 0.1 g kg^{-1}. The first cloud water occurs 5 min after initiation. The cloud base was below 0.5 km, with P = 984.5 hPa and T = 12.6°C. Initial cloud ice forms via the depositional growth of the expense of supercooled cloud water (Pidw) at T = –40°C (top left panel). The dominant processes for the formation of snow particles in this cloud's developing phase are the accretion of cloud water by snow (Psacw) and accretion of cloud ice by snow (Psaci). Initial raindrops occur as a result of collision and coalescence with cloud droplets. Raindrops, once formed, continue to grow through the autoconversion of cloud water (Praut) and accretion of snow by rain (Pracs). At 15 min of the simulation, cloud ice and snow coexist in the upper portions of the cloud above –40°C. Probabilistic freezing of rain contributes to formation of graupel (Pgfr). Hail is produced in two updraft regions by accretion of cloud water, rain and snow in the dry growth regime (Pgdry). Since not all of the liquid water collected can be frozen, wet growth of hail (Pgwet) and the shedding of water drops occur. This shedding mechanism in the 0 to –10°C region of the cloud causes a rapid transformation of cloud to rain. Hail melts as it falls into a warmer region, and thus also increases the water content by transforming into rain. As a result of these processes, in the downdraft region the first large raindrops fall at the ground level. The cloud continues its evolution and rapidly enters its most intense stage with the formation of the hail and rain core in the updraft regions (left bottom panel). The dominant production term for snow is accretion of rain by snow (Psacr) that also produces graupel if rain or snow exceeds threshold values. Snow also forms in the frontal upper portions of the cloud mainly by accretion of cloud water (Psacw) in cold temperature regions. Rainfall is most intense ahead of the storm front and falls over a wider area in two distinct zones. Ice crystals also form rapidly when the plume of the storm spreads at the higher level in the later stage of the storm's development (from 50 to 70 min of the simulation time). The role of microphysics on the pattern of precipitation and the effects of running a different cloud initialization on the pattern of precipitation are evident comparing the cloud physics processes simulated in the model and mean transfer production rates for hydrometeors averaged over 3-h simulation period starting at 1100 UTC (Fig. 11). It is evidenced that accretion of cloud water and rain (Psacw, Psacr) and transfer rate of cloud ice to snow through Bergeron process embryos (Psfi) give a larger contribution to production term for snow under Milano initialization relative to both Cuneo initial meteorological profile and using double sounding initialization. At temperature $T \geq T_0$, accretion of cloud water by snow produces rain and also enhances snow and graupel melting. Hail is mainly produced via wet and dry regime of graupel (Pgwet, Pgdry) as well as through accretion of cloud water and snow by graupel (Pgacw, Pgacs). A relatively larger contribution to rain production under this initialization comes from the accretion of snow by rain (Pracs) and melting of snow (Psmlt). Cloud model simulation employing Milano sounding data has shown a relatively larger accretion rates of cloud water and rain by snow (Psacw, Psacr), accretion of cloud water and rain by graupel (Pgacw, Pgacr), dry growth of graupel (Pgdry) and graupel melting (Pgmlt) compared to Cuneo run. Cloud model simulation using Milano sounding has indicated a slight increase in second ice crystals production Pn2d (Hallet-Mossop ice multiplication) relative to Cuneo run. Results are slight different when we are applying the cloud model algorithm which uses a two upper air soundings. Here we get slightly larger production rates of autoconversion of rain, snow and graupel (Praut, Psaut, and Pgaut) relative to single cell cloud initialization. A relatively higher production rates are noted also in some accretion processes such as: accretion of graupel by cloud water and cloud ice (Pgacw and Pgaci). Snow melting (Psmlt) using two soundings has for about 2 times greater contribution to rain formation relative to Milano case. Transfer rate of cloud ice to snow through Bergeron process embryos which occurs under supersaturation with respect to ice (Psfi) indicates for about

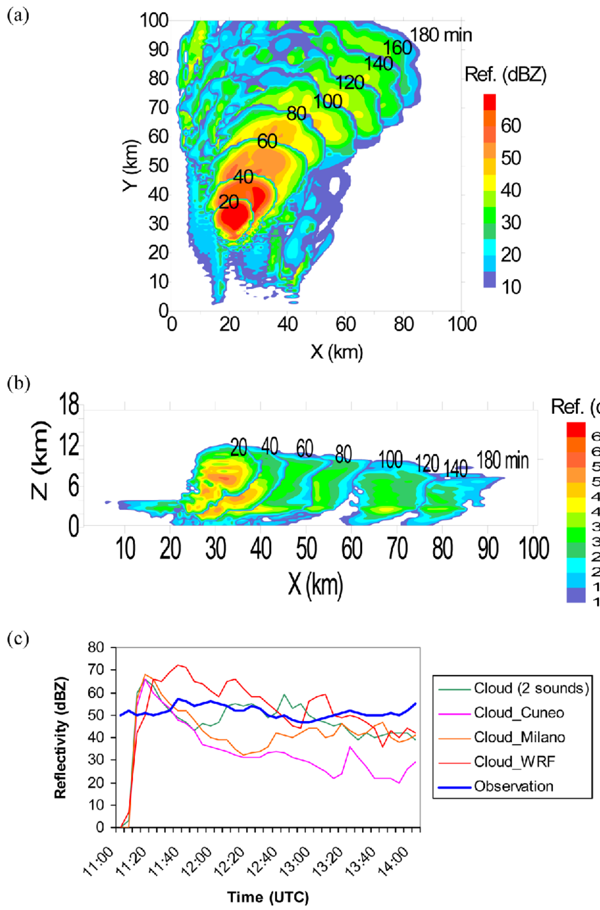

Fig. 12. (a) Horizontal transects of reflectivity at 2.25 km height during simulation time, (b) Same as Fig. 11a but for the vert. transects along SW-NE orientation, and (c) Time evolution of the maximum simulated radar reflectivity (dBZ) averaged over simulation time under different model initialization.

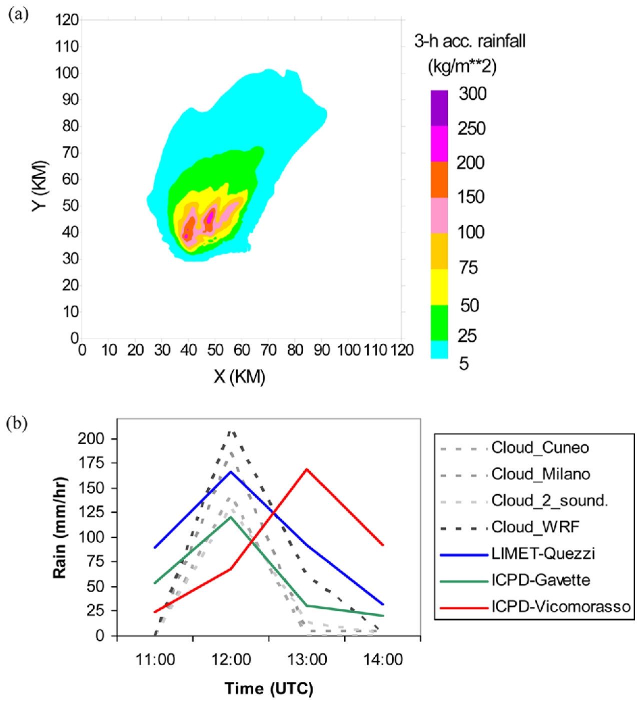

Fig. 13. (a) Model simulated accumulated rainfall (mm) (b) Time evolution of the accumulated rainfall (mm) simulated by cloud model employing a different initialization, WRF v3.6 with 1 km resolution and comparison with observation provided by ICPD official weather network at two rain gauges Gavette and Vicomorasso and one from the semi-professional network LIMET PWS at station Quazzi located in Fereggioano sub-basin close to Genoa.

twice larger efficient production rate compared to single sounding runs. Finally, WRF initialization, results in increased production rates almost in all physical processes simulated in the model, with respect to previous simulations. In overall, the dominant microphysical processes which leads to significant improvement of the QPF in terms of the value of the peak rainfall are the accretion of snow by rain with about ten times greater calculated amount for the averaged production rate (Psacr = $1.1e^{-03}$) compared to other initializations. In addition, the probabilistic freezing of rain to form graupel (Pgfr = $6.6e^{-04}$), accretion of rain by cloud ice and graupel (Piacr = $4.4e^{-04}$; Pgacr = $5.0e^{-04}$), dry and wet growth of graupel (Pgdry = $5.0e^{-04}$; Pgwet = $6.3e^{-04}$) also contribute in enhanced production rates. It is also evident that melting of graupel with an averaged production rate of (Pgmlt = $-2.4e^{-04}$) is for about ten times greater amount than for the other runs.

c. Radar reflectivity fields

Both horizontal and vertical cross-sections of radar reflectivity are simulated with the cloud model. The time evolution of the horizontal cross sections of reflectivity at 2.0 km height illustrated in Fig. 12a indicates that individual thunderstorm cells tend to travel with the mean wind in the cloud-bearing layer. The cell merging along the leading edge of the convective system occurs prior to the MCS's rapid strengthening and the production of the most significant rainfall. The cloud model simulation showed some similarities with the observed structure of the convective cell originated from the MCS. The vertical cross-section of reflectivity along the storm axis (Fig. 12b) provides a more detailed view of the storm's structure and evolution. The convective line includes both continuous echoes at the leading edge of the squall line that have cores with peak reflectivity in developing stage from 20 to 40 min. In the most intense phase of evolution, the reflectivity maps show a convective structure with the maximum reflectivity from 30 to 55 dBZ and 7.5 km vertical extension. After 40 min of the simulation, the storm exhibits a much more uniform vertical reflectivity profile with a narrow band and homogeneous reflectivity in the horizontal plane, with reflectivity from 35 to 50 dBZ. Figure 12c shows time evolution of maximum radar reflectivity (dBZ) over simulation time, using four different cloud model initializations. Based on Rebora et al. (2013) the observed radar reflectivity was above a 40 dBZ threshold for more than 4 hours. As it is depicted in Fig. 2a -

all model runs with exception to that initialized with Cuneo sounding, have more or less correctly captured observed radar reflectivity for more than 2 hours. The numerical simulation with WRF initialization shows higher reflectivity values which are typical for extreme rainfall intensity range of 205 to 421 mm h^{-1} based on the NOAA dBZ scale for weather radar.

d. Analysis of the heavy rainfall

The simulated accumulated rainfall pattern using WRF model initialization, illustrated on Figure 13a shows a very similar shape relative to the observed one depicted on Fig. 1a. One sees, formation of a two isolated rainfall patterns in 20 min. after the storm's initiation, when a new rear-flank updraft and downdraft core was generated. The merging of convective cells increased the storm's intensity and transformed it into a Heavy Precipitation (HP) convective storm. A short (less than 20 min), heavy precipitation period occurred during the simulation with rain intensity of 211 mm hr^{-1}. The total accumulated rainfall within 3-h simulation reaches about 276 mm. Although it is relatively difficult at first glance to identify remarkable differences, there are some differences in the microphysical structure. The cloud model was able to provide a more realistic quantitative estimation of the rainfall intensity in the peak rainfall period from 1100 to 1400 UTC. Figure 13b displays the time evolution of the modelled versus observed, hourly rainfall at a three rainguage stations. The temporal evolutions show a similar pattern with the observations. In general two major peaks registered at ICPD Gavette and LIMET PWS Quezzi stations are well reproduced by all model configurations, even though the rainfall intensity differs in rainfall intensity and timing to some extent with ICPD Vicomerasso station. WRF initialization simulated amount of about 276 mm total 3 hours accumulated rainfall from 1100 to 1400 UTC on 4 November 2011 during most intense phase of convective cell evolution. This result agrees well with the total accumulated precipitation amount measured at the station Fereggiano registered from 1200 to 1500 UTC (see Figs. 1a, b). It is interesting that other cloud model initializations also provide a quite good result that is more or less similar with observed 3-h rainfall amount at the station Gavette.

4. Conclusions

In the present study we investigated the capability and performance of three-dimensional cloud model in simulation of the heavy rainfall event over Genoa on 4 November 2011. The local maximum of observed rainfall was more than 500 mm in a few hours period. Initial set of experiments were carried out using WRF v3.6 atmospheric mesoscale model with employing a different configuration and model setup in three selected domains. A series of quantitative precipitation forecasts for 24 and 3-h period are initialized using NCEP FNL 6 hourly initial and boundary conditions. Results for almost all experiments indicate that WRF model tends to underpredict the total accumulated daily rainfall amount. The cloud permitting simulations with 1 km horizontal resolution and explicit treatment of convection (without parameterization) show advantage in forecast of the maximum accumulated rainfall and capture the pattern structure but the result was also not quite well in respect to spatial placement of the precipitation and accurate amount of rainfall relative to observations. A major focus of this study was to exploit the cloud model potential in simulation of the convective cell evolved from a MCS during the most intense phase from 1200 to 1400 UTC when peak rainfall occurs. Our main objective in the research is to test the cloud model ability and performance in simulation of this particular case. For that purpose a set of sensitivity simulations under different model initializations have been conducted. Given the unstable atmospheric conditions (moist troposphere, strong directional wind shear in a deep layer) the cloud model simulates a strong convective storm that produced heavy rainfall in the span of around 3 hours. The results also indicate that the merging process apparently alters the physical processes through low- and middle-level forcing, increasing cloud depth, and enhancing convection. The examination of the microphysical process simulated by the model indicates that dominant production terms are the accretion of rain by graupel and snow, probabilistic freezing of rain to form graupel and dry and wet growth of graupel. Experiment under WRF v3.6 model initialization has shown some advantage in simulation of the physical processes responsible for production and initiation of heavy rainfall compared to other model runs. Most of the precipitation came from ice-phase particles-via accretion processes and the graupel melting at temperature $T_0 \geq 0^oC$. The available resolved radar images show some similar reflectivity patterns with observation from 1200 to 1400 UTC when the convective cell reaches the most intense phase. The rainfall intensity and accumulated rainfall calculated by the model of 275 mm for 3-h simulation closely reflect the amount of rainfall recorded at station Fereggiano located to the Genoa. Thus, the main benefit is to better resolve convective showers or storms which, in extreme cases, can give rise to major flooding events. In such a way, this model may become major contributor to improvements in weather analysis and small-scale atmospheric predictions and early warnings of such sub-scale processes.

These findings are very important, both as a source of more extended knowledge of such convective scale processes, as well as for documenting the value of the cloud model and its ability to simulate some dynamical and microphysical processes of connective cell originated from MCS and triggering factors for acceleration of the system development and initiation of heavy convective rainfall and flooding. However our conclusion of this study is limited because we focused on this idealized single case study. We hope that with a more extensive experimental work this type of idealized study along with more sensitivity tests to the microphysics sounds like a potentially useful avenue for our future work.

Acknowledgements. First of all, the authors express their gratitude to Dr. Antonio Parodi from CIMA Research Foundation for providing of radar and rainfall data for the convective case experiment related to the Genoa storm flooding. We gratefully acknowledge and appreciate the valuable contributions of Mr. Alessandro Fuccello and Teodoro La Rocca from the Italian Meteorological Service for providing synoptic material and other data associated with this MCS that occurred over Genoa. We would also like to thank Wyoming University for providing the initial upper air sounding data used to run the model. The authors acknowledge the Korean Meteorological Society for supporting the publication fee.

Edited by: Jong-Jin Baik

References

Bedrina, T., A. Parodi, A. Quarati, and A. Clematis, 2012: ICT approaches to integrating institutional and non-institutional data services for better understanding of hydro-meteorological phenomena. *Nat. Hazards Earth Syst. Sci*., **12**, 1961-1968.

Blamey, R. C., and C. J. C. Reason, 2009: Numerical simulation of a mesoscale convective system over the east coast of South Africa. *Tellus*, **61A**, 17-34.

Bresson, E., V. Ducrocq, O. Nuissier, D. Ricard, and C. de Saint-Aubin, 2012: Idealized numerical simulations of quasi-stationary convective systems over the Northwestern Mediterranean complex terrain. *Quart. J. Roy. Meteor. Soc.,* **138**, 1751-1763.

Buzzi, A., S. Davolio, P. Malguzi, O. Drofa, and D. Mastrangelo, 2013: Heavy rainfall episodes over Liguria of autumn 2011: Numerical forecasting experiments. *Nat. Hazards Earth Syst. Sci. Discuss*., **1**, 7093-7135.

Byun, U-Y., J. Hong, S.-Y. Hong, and H. H. Shin, 2015: Numerical simulation of heavy rainfall over central of Korea on 21 September 2010 using the WRF model. *Adv. Atmos. Sci*., **32**, 855-869.

Chen, S. S., Houze, R. A., and B. E. Mapes, 1996: Multiscale variability of deep convection in relation to large-scale circulation in TOGA COARE. *J. Atmos. Sci.,* **53**, 1380-1409.

Clark, P. A., K. A. Browing, C. J. Morcrette, A. M. Blyth, R. M. Forbes, B. Brooks, B., and F. Perry, 2013a: The evolution of an MCS over southern England. I: Observations. *Quart. J. Roy. Meteor. Sci*., **140**, 439-457.

______, ______, R. M. Forbes, C. J. Morcrette, A. M. Blyth, and H. W. Lean, 2013b: The evolution of an MCS over southern England. II: Model simulations and sensitivity to microphysics. *Quart. J. Roy. Meteor. Sci*., **140**, 458-479.

Coniglio, M. C, E. Harold, S. J. Brooks, S. Weiss, and F. Corfidi, 2007: Forecasting the Mainte-nance of Quasi-Linear Mesoscale Convective Systems. *Wea. Forecasting*, **22**, 556-570.

Ćurić, M., 2000: *Cloud dynamics*. Belgrade University Serbia Press, 250 pp.

______, and D. Janc, 1995: On the sensitivity of the continuous accretion rate equation used in bulk-water parameterization schemes. *Atmos. Res*., **39**, 313-332.

______, and ______, 1997: On the sensitivity of hail accretion rates in numerical modeling. *Tellus*, **49**, 100-107.

______, and ______, 2012: Differential heating influence on hailstorm vortex pair evolution. *Quart. J. Roy. Meteor. Soc*., **138**, 72-80.

______, ______, and V. Vučković, 2009: The influence of merging and individual storm splitting on mesoscale convective system formation. *Atmos. Res.*, **93**, 21-29.

De Lima, E., E. L. Nascimento, and K. K. Droegemeier, 2005: Dynamic Adjustment in a Numerically Simulated Mesoscale Convective System: Impact of the Velocity Field. *J. Atmos. Sci*., **63**, 2246-2268.

Doswell, C. A., H. E. Brooks, and R. A. Maddox, 1996: Flash flood forecasting: An ingredients-based methodology. *Wea. Forecasting*, **11**, 560-581.

Durran, D. R., 1981: *The Effects of Moisture on Mountain Lee Waves*. Ph.D. Thesis, Masschussets Institute of Technology, (NTIS PB 82126621).

Goyens, C., D. Lauwaet, M. Schröder, M. Demuzere, V. Lipzig, and P. M. Nicole, 2012: Tracking mesoscale convective systems in the Sahel: relation between cloud parameters and precipitation. *Int. J. Climatol.*, **32**, 1921-1934.

Fiori, E., A. Comellas, L. Molini, N. Rebora, F. Siccardi, D. J. Gochis, S. Tanelli, and A. Parodi, 2014: Analysis and hindcast simulations of an extreme rainfall event in the Mediterranean area: The Genoa 2011 case. *Atmos. Res.,* **138**, 13-29.

Fritsch, J. M., and G. S. Forbes, 2001: Mesoscale convective systems. In *Severe Convective Storms.* Amer. Meteor. Soc., 323-357.

Hsie, E-Y., R. D. Farley, and R. D. Orville, 1980: Numerical simulation of ice-phase convective cloud seeding. *J. Appl. Meteorol*., **19**, 950-977.

Houze, R. A., 1993: *Cloud Dynamics*. Academic Press, 573 pp.

______, 2004: Mesoscale convective systems. *Rev. Geophys*., **42**, doi:10. 1029/2004RG000150.

Klemp, J. B., and D. R. Durran, 1983: An upper boundary condition permitting internal gravity wave radiation in numerical mesoscale models. *Mon. Wea. Rev.,* **111**, 430-444.

______, and R. B. Wilhelmson, 1978: The simulation of three-dimensional convective storm dynamics. *J. Atmos. Sci*., **35**, 1070-1096.

Lin, Y. L., R. D. Farley, and H. D. Orville, 1983: Bulk parameterization of the snow field in a cloud model. *J. Climate Appl. Meteor.,* **22**, 1065-1092.

Marsham, J. H., and D. J. Parker, 2006: Secondary initiation of multiple bands of cumulonimbus over southern Britain. Part II. Dynamics of secondary initiation. *Quart. J. Roy. Meteor. Sci*., **132**, 1053-1072.

Mathon, V., L. Henri, and L. Thierry, 2002: Mesoscale Convective System Rainfall in the Sahel. *J. Appl. Meteor.,* **41**, 1081-1092.

Mrowiec, A. A., C. Rio, A. M. Fridlind, A. S. Ackerman, A. S. Del Genio, O. M. Pauluis, A. C. Varble, and J. Fan, 2012: Analysis of cloud-resolving simulations of a tropical mesoscale convective system observed during TWP-ICE: Vertical fluxes and draft properties in convective and stratiform regions*. J. Geophys. Res*., **117**, D19201, doi: 10.1029/2012JD017759.

Nachamkin, J. E., and W. R. Cotton, 1999: Interactions between a Developing Mesoscale Convective System and Its Environment. Part II: Numerical Simulation. *Mon. Wea. Rev.*, **128**, 1225-1244.

Nakazawa, T., 1988: Tropical cloud clusters within intraseasonal variations over the western Pacific. *J. Meteor. Soc. Japan*, **66**, 823-839.

Orville, H. D., and F. J. Kopp, 1977: Numerical simulation of the history of a hailstorm. *J. Atmos. Sci.,* **34**, 1596-1618.

Parodi, A., G. Boni, L. Ferraris, F. Siccardi, P. Pagliara, E. Trovatore, E. Foufoula-Georgiou, and D. Kranzlmueller, 2012: The “perfect storm”: from across the Atlantic to the hills of Genoa. *EOS*., **93**, 225-226.

Parker, M. D., and R. H. Johnson, 2004: Structures and Dynamics of Quasi-2D Mesoscale Convective Systems. *J. Atmos. Sci.,* **61**, 545-567.

Pulvirenti, L., M. Chini, S. Marzano, N. Pierdicca, S. Mori, L. Guerriero, G. Boni, and L. Candela, 2011: Detection of floods and heavy rain using Cosmo-SkyMed data: The event in Northwestern Italy of November 2011. *2012 IEEE Int. Geosci. Remote Sens. Symp*., Munich, 3026-3029.

Rebora, N., and Coauthors, 2013: Extreme Rainfall in the Mediterranean: What Can We Learn from Observations? *J. Hydrometeor*., **14**, 906-922.

Schenkman, A. D., M. Xue, and A. Shapiro, 2012: Tornadogenesis in a Simulated Mesovortex within a Mesoscale Convective System. *J. Atmos.*

Sci., **69**, 3372-3390.

Smith, P. L., G. G. Myers, and H. D. Orville, 1975: Radar reflectivity calculations on numerical cloud models using bulk parameterization of precipitation. *J. Appl. Meteor.,* **14**, 1156-1165.

Sekhon, R. S., and R. C. Srivastava, 1970: Snow size spectra and radar reflectivity. *J. Atmos. Sci*., **27**, 299-307.

Silvestro, F., S. Gabellani, F. Giannoni, A. Parodi, N. Rebora, R. Rudari, and F. Siccardi, 2012: A hydrological analysis of the 4 November 2011 event in Genoa. *Nat. Hazards Earth Syst. Sci*., **12**, 2743-2752.

Spiridonov, V., and M. Ćurić, 2003: Application of a cloud model in simulation of atmospheric sulfate transport and redistribution. Part I: Model description. *Idojárás*, **107**, 85-115.

______, and ______, 2006: A three-dimensional modeling studies of hailstorm seeding. *J. Wea. Mod*., **38**, 31-37.

______, Z. Dimitrovski, and M. Ćurić, 2010: A Three-Dimensional Simulation of Supercell Convective Storm. *Adv. Meteor*., **2010**, doi: 10.1155/2010/234731.

Telenta, B., and N. Aleksic, 1988: A three-dimensional simulation of the 17 June 1978 HIPLEX case with observed ice multiplication. *2nd International Cloud Modeling Workshop*, Toulouse, WMO/TD No. **268**, 277-285.

van Weverberg, K., and Coauthors, 2013: The Role of Cloud Microphysics Parameterization in the Simulation of Mesoscale Convective System Clouds and Precipitation in the Tropical Western Pacific. *J. Atmos. Sci.,* **70**, 1104-1128.